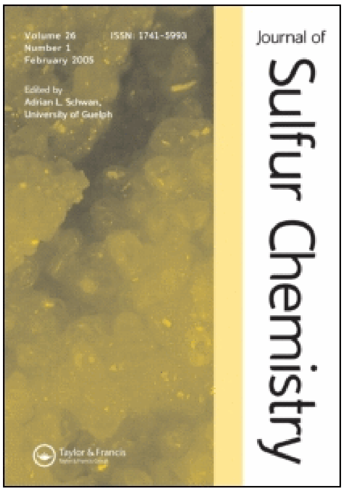

Journal of Sulfur Chemistry
Publication details, including instructions for authors and subscription information:
http://www.informaworld.com/smpp/title~content=t713926081

Comparison of the structural properties of compounds containing the XSSX moiety (*X* = H, Me, R, Cl, Br, F, OR)

Eli Zysman-Colman; David N. Harpp

To cite this Article Zysman-Colman, Eli and Harpp, David N.(2004) 'Comparison of the structural properties of compounds containing the XSSX moiety (*X* = H, Me, R, Cl, Br, F, OR)', Journal of Sulfur Chemistry, 25: 4, 291 — 316
To link to this Article: DOI: 10.1080/17415990410001710163
URL: http://dx.doi.org/10.1080/17415990410001710163

J. Sulfur Chemistry
Vol. 25, No. 4, August 2004, 291–316

REVIEW

Comparison of the structural properties of compounds containing the XSSX moiety ($X =$ H, Me, R, Cl, Br, F, OR)

ELI ZYSMAN-COLMAN and DAVID N. HARPP*

Department of Chemistry, McGill University, 801 Sherbrooke St. W., Montreal,
Quebec, Canada, H3A 2K6

(*Received 24 February 2004; In final form 4 April 2004*)

A comparison of the structural parameters of a wide variety of compounds containing the S−S bond is summarized.

1. Introduction

The S−S single bond is a ubiquitous unit in structural biology, being essential for the activity in a diversity of proteins, of which insulin, oxytocin and vasopressin [1, 2], ribonuclease A, phospholipase A_2 and immunoglobins are illustrative [3]. One reason why Nature uses the S−S bond in conferring structural rigidity is the high bond energy of this functionality, which at *ca*. 63 kcal mol^{-1} is the third strongest homonuclear single bond [4]. Nevertheless, it is considered a weak bond compared with other bonds that normally break in chemical reactions. Apart from serving to tailor the three-dimensional structure of proteins, disulfide bonds appear in rubber vulcanization [5], drugs [6] such as Antabuse (TETD) [7], molecules used in marine organisms [8, 9], and as aqueous gelators [10].

To best understand and provide a context for the conformational analysis and theoretical calculations highlighted in this review, a detailed investigation of the geometries of related disulfides, HSSH, ClSSCl, BrSSBr, FSSF and dialkoxy disulfides is presented. Geometries for all these compounds are defined according to figure 1.

The origin of the S−S barrier to rotation will also be explored as well as a comparison of experimental and theoretical work to determine the minimum level of theory needed to accurately describe these systems.

2. HSSH system

The geometry of dihydrogen disulfide HSSH (**1a**) as well as its isotopic derivatives has been determined by electron diffraction [11] and microwave spectroscopy [12–20]. Often with the geometry given by microwave spectroscopy (MW), the parameters are recalculated from the

---

* Corresponding author. E-mail: david.harpp@mcgill.ca

J. Sulfur Chemistry
ISSN 1741-5993 print; ISSN 1741-6000 online © 2004 Taylor & Francis Ltd
http://www.tandf.co.uk/journals
DOI: 10.1080/17415990410001710163

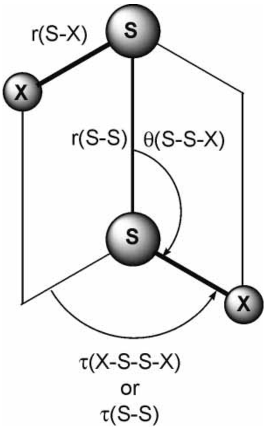

Figure 1. Structural parameters for XSSX systems. Bond lengths are defined as r(S−S) and r(S−X), bond and dihedral angles are defined as θ(S−S−X) and τ(S−S) respectively.

same data set and then re-reported. Disulfane (**1a**) has an analogous structure to that of HOOH (**2a**). Selected experimental structural parameters are highlighted in table 1.

Initial work [12, 13] underestimated both the r(S−H) bond length and θ(H−S−S) bond angle. This is most likely because the authors based their microwave geometries on flawed electron diffraction [11] data that served as a reference for the θ(H−S−S) bond angle. In general, the location of hydrogen atoms in the presence of heavier atoms is problematic by diffraction techniques. Given that bond lengths derived from rotational constants are correlated to the bond angle, an inappropriate determination of the latter parameter will thus affect the two former; torsional angles are weakly correlated with other structural parameters and remain consistent throughout. The average bond angle of 95.8° is slightly larger than that of H_2S (92.2°) [22] but is substantially smaller than that for alkyl or halogenated disulfides (*vide infra*). The small bulk of the hydrogen atoms and the subsequent decrease in H−H and S−S repulsions may explain this smaller bond angle.

Theoretical modeling of this system proves quite accurate, even with smaller basis sets, as summarized in table 2; the inclusion of polarization functions on heavy atoms is essential for determining accurate parameters [23, 24]. It has also been suggested that addition of correlation corrections is required to obtain good structural parameters for the analogous H_2O_2 (**2a**) system [25, 26] though this does not seem to be the case here. The bond order for the S−S bond was calculated [27] to be 0.95, an indication of the single bond character of this parent compound; thus the covalent radius of sulfur can now be derived as $2.055/2 = 1.03$Å, where we have used the most recent MW [21] S−S bond length.

Bonding in X−S−S−X systems is characterized by a *gauche* conformation about the S−S bond. The bonds formed are almost entirely p in character. Thus there exists a non-bonding

Table 1. Experimentally derived parameters for **1a**.

r(S−S) (Å)	r(S−H) (Å)	θ(H−S−S) (°)	τ(H−S−S−H) (°)	Method	Ref.
2.055 ± 0.001	1.327 ± 0.003	92.00 ± 0.50	90.60 ± 0.10	MW	12
2.055 ± 0.001	1.327 ± 0.003	91.30 ± 0.05	90.60 ± 0.05	MW	13
2.058 ± 0.003	1.345 ± 0.003	98.10 ± 0.30	90.80 ± 0.30	MW	20
2.0611 ± 0.0001	1.3410 ± 0.0003	97.42 ± 0.04	90.75 ± 0.05	MW	19
2.055		98.10	89.60	MW	21
2.056	1.342	97.90	90.30	MW	18
2.057 ± 0.002	1.336 ± 0.009	95.80 ± 3.23	90.44 ± 0.45	Average	

Table 2. Calculated structural parameters for **1a**.

r(S–S) (Å)	r(S–H) (Å)	θ(H–S–S) (°)	τ(H–S–S–H) (°)	Method	Ref.
2.081	1.356	98.3	91.7	SCF/DZ + P	28
2.063	1.336	98.9	90.3	SCF/3-21G^*	29
1.958	1.327	99.1	88.1	*ab initio* STO-3G*	30
2.067	1.331	98.2	89.7	SCF-CI/DZ + P	31
2.066	1.327	98.6	89.9	MP2/4-31G*	32
2.066	1.328	99.0	90.0	HF-SCF/6-31G*	27
2.063	1.327	99.1	89.8	HF/6-31G*	33
2.070	1.333	98.7	90.5	MP2/6-31G**	34
2.082	1.336	98.1	90.4	MP2/6-311G**	35
2.092	1.333	97.5	90.8	MP2/6-311G(2d,2p)	34
2.092	1.333	97.5	91.2	MP2/6-311G++(2d,2p)	34
2.064	1.338	97.8	91.0	MP2/6-311G++(2df,2p)	34
2.067	1.343	98.0	90.7	CCSD(T)/cc-pVQZ	36
2.064	1.334	98.4	90.3	Average [37]	
0.034	0.008	0.6	0.9	Error	

electron pair that resides in a perpendicular 3p orbital on each sulfur atom (figure 2). The size of these orbitals leads to a partial overlap of these MOs. The lone pair-lone pair repulsion inherently caused by the formed π- and π^*-MOs results in a destabilization (and subsequent lengthening) of the S–S bond that is maximized when $\tau = 0$ and 180°; this destabilization is diminished when $\tau = 90°$ and $\tau = -90°$ due to the orthogonality of the two 3 p orbitals. The splitting of AOs to form MOs is asymmetric [38] [illustrated in figure 3(a)].

As a corollary to this MO argument, when H_2S_2 (or any other XSSX system) is in the *gauche* conformation there is a maximum stabilizing overlap that occurs with each of the lone pair 3p orbitals to that of the adjacent S–H (or S–X as the case may be) σ^* MO (figure 3b). The above MO description is indicative of a hyperconjugative mechanism. Mulliken [39] population analyses show that the largest S–S overlap population does occur at this (*ca.* 90°) dihedral

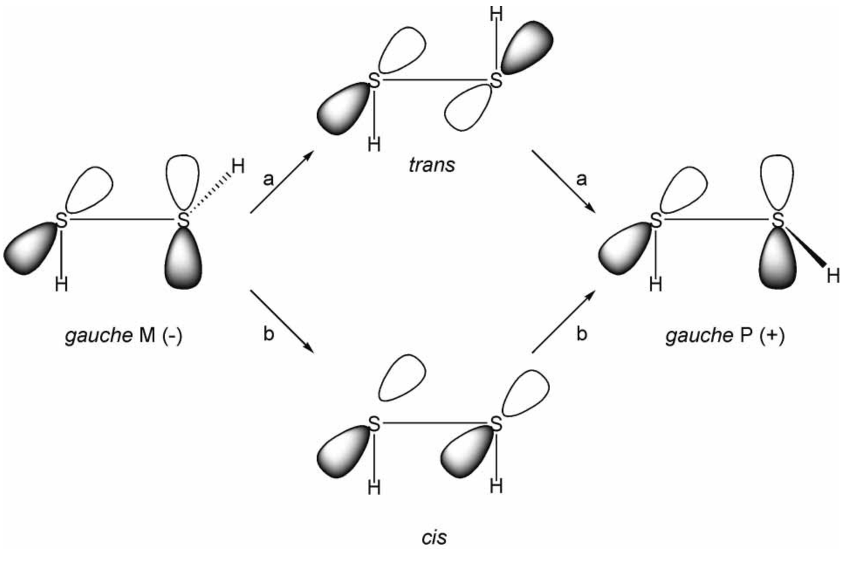

Figure 2. 3p orbital orientation in the ground and cis and trans transition states.

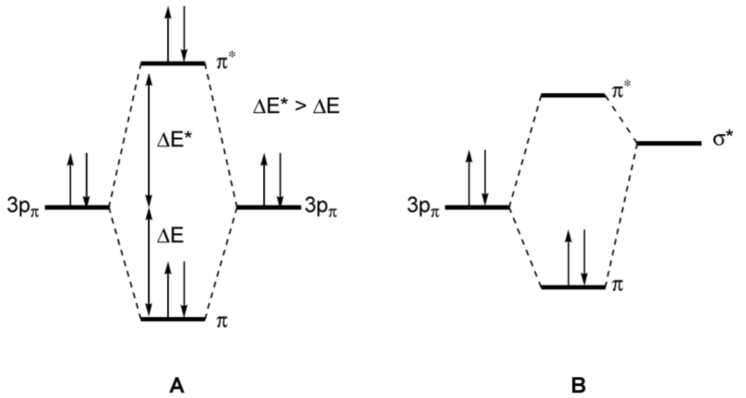

Figure 3. (a) Splitting of adjacent S-3p$_\pi$-orbitals. (b) Splitting of S-3p$_\pi$-orbital with that of an adjacent S−X antibonding orbital. The magnitude of the splitting in each case depends on the dihedral angle τ and on the origin of X.

angle, thus indicating that the total energy of the compound is lowest [40]. For these reasons, the observed dihedral angle in **1a** is *ca.* 90° which represents an energy minimum for the compound. Thus there are two energetically degenerate conformations of **1a** that are antipodal in the S−S unit. While the XSSX systems are inherently chiral, they remain optically inactive and unresolvable if the substituent X is achiral and the magnitude of the S−S rotational barrier is sufficiently low.

The geometries of the cis and trans transition state structures in figure 2 indicate distortions from the ground state geometry. The calculated r(S−S) is *ca.* 0.04–0.05 Å longer and the θ(S−S−H) is 1° and 4° smaller respectively while r(S−H) remains essentially unchanged [31]. Such changes are not unusual and similar results have been observed in sulfur homocycles wherein $\tau = ca.\ 0°$ [41].

The barrier to rotation about the S−S bond of course also depends on the dihedral angle due to the same molecular orbital considerations (*vide supra*). Although there is much variation in the measured and calculated barriers (table 3), the cis barrier (*via* path **b** in figure 2) is consistently higher than that of the trans barrier (*via* path **a** in figure 2). Some of this variation may be caused by the use of inaccurate structural parameters as well as the assumption that rotation is rigid (that is all other bond angles are constrained as the energies are calculated during the rotational profile about the S−S bond). Others did not optimize transition state geometries prior to obtaining single point energies. In general, *ab initio* calculations can reproduce many rotational barriers at the HF level given the use of a large enough basis set [42]; the lack thereof is evident in the barriers calculated by Laitinen (geometry optimization using the same method was also poor) [43]. Inclusion of electron correlation did not change the barrier heights [19, 31]. Notably, full optimization of the energy surface using appropriately large basis sets is standard in modern theoretical work for rotational barriers. Thus the HF predictions of Samdal [33] and co-workers (last entry of table 3) should be viewed as the most accurate.

The increased height of the cis barrier is most probably due to a relatively decreased stabilizing hyperconjugative $\sigma_{S-H} \rightarrow \sigma^*_{S-H}$ interaction (similar to that found in ethane [46–49]) as compared with the trans transition state [50]. The slightly lower calculated trans barrier as compared with the measured barriers (which as a matter of course are in fact measurements of the trans barrier) is due to geometry relaxation [45]. The barrier height is also a function of the van der Waals radii and the electronegativities of the respective atoms about the X−X bond (in this case S−S). This is illustrated in table 4 wherein moving from a first row element to one in the second row may lead to a decreased barrier but this effect can be compensated by moving from left to right across the periodic table.

A more important comparison is that between HO−OH (**2a**) and HS−SH (**1a**). The barriers for **2a** are shown in table 5.

Table 3. Measured and calculated barriers to rotation about the S−S bond in **1a**.

Measured (kcal mol^{-1})	Calculated (kcal mol^{-1}) cis	trans	Δ[a] (kcal mol^{-1})	Method	Ref.[b]
6.9			–	Far IR	14
[c]			–	Millimeter wave	12
	9.3	6.0	3.3	SCF[d]	44
	1.5	0.9	0.6	EH	40
	6.4	3.5	2.9	STO-3G	30
	12.5	10.8	1.7	STO-3G*	30
	9.0	5.2	3.8	HF-SCF[e]	45
	8.7	6.1	2.6	SCF/3-21G*	29
	7.6	5.1	2.5	SCF/ZPE	31
	7.5	5.0	2.5	CI-SD/ZPE	31
	22.5	4.1	18.4	MINI-1	43
	26.4	14.3	12.1	MINI-1*	43
	7.7	5.1	2.6	SCF[d]	19
	7.8	5.0	2.8	MP2//SCF	19
8.2			–	IR	21
	8.1	5.8	2.3	MW	18
	8.4		–	HF/STO-3G(M3*)	27
	8.5	6.1	2.5	HF/6-31G*	33

[a] Difference between cis and trans barriers. [b] References are in chronological order. [c] No value determined but authors quote almost equal barriers. [d] Included the use of a double ζ basis set augmented by polarization functions. [e] Included the use of an extended polarized basis set.

Table 4. Barriers to rotation about C−X bonds where X = C, Si, N, P, O, S.

Compd	Barrier[a] (kcal mol^{-1})	Compd	Barrier[a] (kcal mol^{-1})	Compd	Barrier[a] (kcal mol^{-1})
CH_3-CH_3	2.93	CH_3-NH_2	1.98	CH_3-OH	1.07
CH_3-SiH_3	1.66	CH_3-PH_2	1.96	CH_3-SH	1.27
Δ = −1.27		Δ = −0.02		Δ = 0.20	

[a] From ref. [51].

Table 5. Calculated barrier to rotation for HOOH (**2a**).

Calculated (kcal mol^{-1}) cis	trans	Δ[a] (kcal mol^{-1})	Method	Ref.[b]
10.9	0.6	10.3	SCF	52
7.3	1.1	6.2	MW	18
9.1	0.9	8.2	HF/6-31G*	33

[a] Difference between cis and trans barriers. [b] References are in chronological order.

A comparison of barrier heights clearly shows that for all cases, except those values reported by Boyd [40], HSSH has the higher trans barrier (by *ca.* 6 kcal mol^{-1}); the cis barrier for both compounds is of a comparable energy. Given that **2a** has a similar geometry ($\tau = ca.115°$) to that of **1a**, the increased trans barrier must be due to an increased lone pair-lone pair repulsion afforded by the larger, more diffuse 3p orbitals of adjoining sulfurs as compared with the

2p orbitals of adjoining oxygens. This results in a 2-fold torsional barrier [53] component for **1a** (the MP2 [19] two-fold component is 3.21 kcal mol^{-1}) that is *ca.* double that of the experimentally [54] determined one in **2a** (1.81 kcal mol^{-1}). Counteracting this two-fold torsional term is the fact that in H_2S_2 (**1a**) there are decreased dipole-dipole and atom–atom interactions and decreased polarity in the S—H bond as compared with the O—H bond [19].

The calculated dipole moments of the transition state and ground state geometries of **1a** are shown in table 6. The indicated difference in gas-phase dipole moments between the trans transition state and the ground state suggests that the barrier to rotation may be solvent dependent.

Table 6. Calculated dipole moments for **1a**.

Calculated dipole moment (D)[a]		
cis	trans	equilibrium[b]
1.82	0.00	1.36

[a]From ref. [45]. [b]Calculated for the ground state geometry – Expt [55] = 1.17 D.

Here, there has been an extensive overview of the geometry and torsional barrier for **1a**. Analysis in the following systems is undertaken to help provide a comparison to the HSSH (**1a**) system.

3. MeSSMe system

The structure of dimethyl disulfide (**3a**) resembles that of **1a**. The structural parameters, both experimental and theoretical, are outlined in table 7.

Table 7. Experimental and theoretical structural parameters for **3a**.

r(S—S) (Å)	r(S—C) (Å)	θ(C—S—S) (°)	τ(C—S—S—C) (°)	Method	Ref.[a]
2.038	1.810	102.8	84.7	MW[b]	56
2.022 ± 0.003	1.806 ± 0.002	104.1 ± 0.3	83.9 ± 0.9	ED	57
2.029 ± 0.003	1.816 ± 0.003	103.2 ± 0.2	85.0 ± 4.0	ED	58
2.030 ± 0.008	1.811 ± 0.005	103.4 ± 0.7	84.5 ± 0.6	Average [37]	
1.842	[c]	103.2	85.0	CNDO/2	59
2.030	1.818	103.7	83.2	MM1	60
2.064	1.809	100.0	90.6	*ab initio* STO-3G	30
1.950	1.803	102.9	87.4	*ab initio* STO-3G*	30
2.050	1.823	102.3	88.4	SCF/3-21G*	29
2.054	1.812	102.1	85.1	MP2/6-31G**	34
2.072	1.819	101.5	84.7	MP2/6-311G(2d,2p)	34
2.064	1.807	100.8	83.7	MP2/6-311G**	35
2.016 ± 0.080	1.813 ± 0.007	102.1 ± 1.2	86.0 ± 2.6	Average [37]	

[a]References chronologically ordered per section. [b]No errors reported. [c]Not determined.

All calculations accurately predict the r(S—C) bond length as well as the bond and $\tau(S—S)$ angles. Most calculations seem to overestimate the experimental r(S—S) by as much as 2% from the average experimental value. This is especially true when electron correlation is added (last three entries). The addition of polarization functions to the STO-3G basis set severely underestimates the r(S—S) bond length. Semi-empirical methods also underestimate r(S—S) though molecular mechanics methods accurately predict the geometry of **3a**. As with **1a**, $r(\text{S}-\text{S})$ is a true single bond and compares favorably with rhombohedral-S_6 ($r(\text{S}-\text{S})[61] = 2.057\text{Å}$) and orthorhombic-$\text{S}_8$ ($r(\text{S}-\text{S})[62] = 2.037\text{Å}$).

The main structural difference between **3a** and **1a** is in the bond angle, which is *ca.* 7° wider in **3a**; whereas $r(\text{S}-\text{S})$ is *ca.* 1% shorter. The widening of the bond angle is ostensibly due to increased Me$-\text{S}_\beta$ repulsive interactions. The intramolecular $r(\text{C}-\text{S})$ of *ca.* 3.0 Å is less than of the sum of the respective van der Waals radii of the constituent atoms (3.4 Å).

Experimental and calculated barriers to rotation for **3a** are reported in table 8.

Table 8. Measured and calculated barriers to rotation about the S$-$S bond for **3a**.

Measured (kcal mol^{-1})	Calculated (kcal mol^{-1}) cis	trans	Δ^a	Method	Ref.[b]
9.5[c]				Raman	63
6.8				Calorimetric data[d]	64
7.3				IR	65
10[e]				Raman	66
	2.9	1.3	1.6	PCILO	67
	45.9	14.5	31.4	ZDO-SCF	68
	7.0	2.2	4.8	EH	40
	17.7	10.8	6.9	CNDO/2	59
	10.6	7	3.6	MM1	60
	18.0	4.4	13.6	STO-3G (rigid rotor)	30
	21.1	12.7	8.4	STO-3G* (rigid rotor)	30
	7.5	2.9	4.6	SCF/3-21G	29
	12.0	5.7	6.3	SCF/3-21G*	29
	11.4	5.7	5.7	HF/6-31G*[f]	15
	11.3	5.5	5.8	HF/6-31G*[f,g]	69
	11.4	6.3	5.1	MP4/6-311G**[g]	69
	11.6	6.1	5.5	MP2/6-31G*[h]	70

[a] Difference between cis and trans barriers. [b] References are in chronological order. [c] Caution: assumed symmetrical barrier shape and neglected effects of coupling between S$-$S rotation and vibrational degrees of freedom in MeSSMe. [d] Estimated from calculated and observed entropy and heat capacity. [e] Approximate value reported. [f] Based on HF/6-31G* optimized geometry. [g] Calculations reported do not include ZPVE correction. [h] Based on MP2/6-31G* optimized geometry.

The best experimental estimates suggest a barrier of *ca.* 7 kcal mol^{-1}. With **3a**, rotation is expected to proceed through a trans transition state. *Ab initio* calculated results seem to converge with larger basis sets (last three entries); however, these seem to underestimate the trans barrier by *ca.* 1 kcal mol^{-1}. Deconvolution of the torsional potential function [71] indicates that the two-fold term (V_2) predominates [69, 72]. Of those reported in the literature, only barriers derived from Allinger's MM1 force field [60] suitably reproduce the experimental results. Evidently, as with **1a**, the addition of polarization functions is essential in barrier determination (contrast last five entries). It is also evident that electron correlation increases the trans barrier slightly (contrast last four entries). The calculated and experimental barriers for **3a** are comparable with those of **1a** (table 3).

The barrier for MeSSH **4** was calculated by Ha at the SCF/3-21G* [29], reporting cis and trans barriers of 8.9 and 5.9 kcal mol^{-1} respectively. Comparing this result to that obtained for **3a** and **1a** suggests that the inclusion of methyl groups increases only the cis barrier and that the trans barrier is defined solely through an electronic interaction (that is the methyl group is not sufficiently bulky to affect this barrier – *vide infra* for examples).

4. Other disulfides with the C$-$S$-$S$-$C moiety

In general, organic disulfides have a similar geometry to that of MeSSMe (**3a**) [73–75]. Table 9 gives the geometries of a representative set of disulfides. Unlike **3a**, the next smallest disulfide, EtSSEt (entry 1), is predicted to show a 1% increase in r(S$-$C); other parameters remaining essentially the same. In fact, this small increase in r(S$-$C) is true with most dialkyl disulfides (where C_α is sp^3 hybridized) and is likely due to the increased steric demands of larger R groups (*cf.* table 9).

One of the shortest registered r(S$-$S)s for a disulfide is 1.999 Å for tetraethylthiuram disulfide (TETD) (entry 6). Even for this molecule, there is only a 1.5% decrease in bond length from that of **3a**; recently the S$-$S linkage of a double helical cyclic peptide (Adm-Cyst)$_3$ was reported [76]; however, the extremely short r(S$-$S) = 1.858 Å warrants caution [77]. The corresponding longest reported r(S$-$S) is 2.110 Å (entry 12). This longer bond (*ca.* 3.5% longer than in **3a**) is almost certainly due to the bulky tris(trimethylsilyl) methyl groups, as is its highly unusual τ(S$-$S) of 180°. Interestingly, whereas entry 12 compensates for the bulky R group through a long S$-$S bond, Tr-SS-Tr (entry 13) does so with the longest reported r(S$-$C) of 1.931 Å.

Dicubyl disulfide (entry 7) has an unusually small τ(S$-$S) for disulfides bearing a tertiary carbon [τ_{av}(S$-$S) $=$ 112.4° from entries 5, 8, 13, 26]. This has been attributed to the strained nature of the cubyl geometry wherein the τ(C$-$S)s are distorted. This enables a minimization of steric interactions between the β-carbon and the S$-$S moiety. The accompanying short r(S$-$C) is *ca.* 5% smaller than the average bond length for a disulfide with a tertiary-substituted carbon. This is a structural manifestation of the high s-character of the C_{cubyl} moiety. This can be seen by comparing r(S$-$C) for this case with those of disulfides containing an sp^2 carbon attached to the S$-$S functionality (entries 11, 14–22). In fact, except for the τ(S$-$S) dihedral angle, the other structural parameters for these cases are unresponsive to substitution changes about the benzene ring that alter the electronics of the respective systems (entry 11 does have an unusually small bond angle). Entry 11 also has one of the smallest τ(S$-$S) and both angle deformations from the ideal are most probably caused by the lack of conformational flexibility afforded by the biphenyl system. Entry 23 also has a massively distorted torsional angle and S$-$S bond length, but entries 11 and 23 are exceptional cases. It is unclear why entries 16-18 and 25 have unusually small τ(S$-$S) (*ca.* 12% smaller than in **3a**) but this may be in part related to the extensive intermolecular hydrogen bonding observed in the solid state (entries 16 and 25).

In general, deviations to smaller angles from an idealized τ(S$-$S) of *ca.* 90 ° are accompanied by a corresponding increase in r(S$-$S). For instance, introduction of the S$-$S moiety into a ring as in 1,2-dithiolane [100] **5** or in natural products bearing the piperazinedione core such as the sporidesmins [101] **6** greatly enhances the lone pair-lone pair repulsion, thereby leading to an increased r(S$-$S).

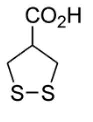

τ = 27°

r(S-S) = 2.096 Å

5

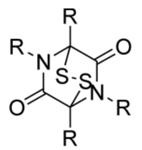

τ = 8.5°

r(S-S) = 2.096 Å

6

Few studies have been carried out on the barrier to rotation about disulfides bearing larger substituents. The results for some disulfides are shown in table 10.

Table 9. Structural parameters of some dialkyl and diaryl disulfides.

Entry	Disulfide	r(S−S) (Å)	r(S−C) (Å)	θ(C−S−S) (°)	τ(C−S−S−C) (°)	Method	Ref.
1	Et-SS-Et	2.038	1.832	103.7	90.0	CNDO/2	78
2	nPr-SS-nPr	2.051	1.830	102.9	−89.3	HF/6-31G*	35
3	Allyl-SS-Allyl	2.052	1.834	103.3	−86.9	HF/6-31G*	35
4	Allyl-SS-nPr	2.066	1.807		84.0	HF/6-31G*	35
5	di-*t*-butyl disulfide	2.029	1.847	106.2	113.8	MM1	79
6	TETD	1.999	1.820 ± 0.030	103.5 ± 0.3	90.0	X-Ray	80
7	Cubyl-SS-Cubyl	2.044 ± 0.001	1.771 ± 0.002	104.6 ± 0.1	−86.5 ± 0.1	X-Ray	81
8	DAD	2.048 ± 0.007	1.840 ± 0.020	107.3 ± 0.6	110.5 ± 0.9	X-Ray	82
9	DAD	2.029	1.845	106.2	113.8	MM1	83
10	Bn-SS-Bn	2.020		103.3	92.0	X-Ray	84
11	2,2′-Biphenyl disulfide	2.050 ± 0.003	1.750 ± 0.010	98.3 ± 0.2	69.0	X-Ray	85
12	$(\mathrm{Me_3Si})_3\mathrm{C{-}SS{-}C(SiMe_3)_3}$	2.110 ± 0.010	1.844 ± 0.002	105.7 ± 0.1	180.0	X-Ray	86
13	Tr-SS-Tr	2.012 ± 0.001	1.931 ± 0.030	110.9 ± 0.1	110.3	X-Ray	86
14	Ph-SS-Ph	2.023 ± 0.001	1.788 ± 0.003	105.9 ± 0.1	90	X-Ray	87
15	2,2′-Dinitrophenyl disulfide	2.045 ± 0.004	1.797 ± 0.009	104.4 ± 0.3	85.1	X-Ray	88
16	3,3′-Dicarboxy-4′4′ dinitrophenyl disulfide	2.023 ± 0.002	1.779 ± 0.005	105.5 ± 0.2	76.0	X-Ray	89
17	4,4′-Dinitrophenyl disulfide	2.019 ± 0.005	1.767 ± 0.010	106.2 ± 0.3	72.0	X-Ray	90
18	Dipentafluorophenyl disulfide	2.059 ± 0.004	1.770 ± 0.007	101.3 ± 0.3	76.5	X-Ray	91
19	2,2′-Diaminophenyl disulfide	2.060 ± 0.003	1.760 ± 0.007	103.3 ± 0.3	90.5	X-Ray	92
20	Di-2-pyrimidyl disulfide dehydrate	2.016 ± 0.001	1.781 ± 0.002	104.7 ± 0.1	82.5	X-Ray	93
21	Di-2-pyridyl disulfide	2.016 ± 0.002	1.785 ± 0.002	105.7 ± 0.1	87.1	X-Ray	87
22	3,3′-Dihydroxydi-2-pyridyl disulfide	2.018 ± 0.001	1.785 ± 0.002	104.8 ± 0.7	93.2	X-Ray	94
23	5-[1-(2′-Deoxy-α-D-ribofuranosyl)uracilyl] disulfide	2.108 ± 0.003	1.756 ± 0.007	102.0 ± 0.2	50.0	X-Ray	95
24	4-[1-(α-D-Ribofuranyl)uracilyl] disulfide	2.022 ± 0.004	1.790 ± 0.020	104.0 ± 0.4	87.0	X-Ray	96
25	5-(1-Methyluracil) disulfide	2.074 ± 0.003	1.750 ± 0.010	100.7 ± 0.3	78.0	X-Ray	97
26	D-Penicillamine disulfide	2.049	1.866	105.5	115.0	X-Ray	98
27	L-Cysteine hexagonal	2.032 ± 0.004	1.820 ± 0.012	114.5 ± 0.3	106.0 ± 1.0	X-Ray	99

Table 10. Calculated and measured barriers to rotation for some disulfides.

Entry	Disulfide	Measured (kcal mol^{-1})	Calculated (kcal mol^{-1}) cis	Calculated (kcal mol^{-1}) trans	$\triangle^{a}$ (kcal mol^{-1})	Method	Ref.
1	Diethyl disulfide		19.5	5.1	14.4	STO-3G	30
2	Diethyl disulfide		12.2	7	5.2	MM1	102
3	*t*-Butyl methyl disulfide		17.2	6.6	10.6	MM1	102
4	*t*-Butyl ethyl disulfide		17.7	6.6	11.1	MM1	102
5	*t*-Butyl i-propyl disulfide		19.6	6.7	12.9	MM1	102
6	Di-*t*-butyl disulfide		28.8	5	23.8	MM1	102
7	Di-*t*-butyl disulfide			6		B3LYP/6-31G*[b]	81
8	Dicubyl disulfide			5.2		B3LYP/6-31G*[b]	81
9	DAD (di-*tert*-adamantyl disulfide)		29.7	5.3	24.4	MM1	83
10	Benzyl trichloromethyl disulfide	9.4[c]				DNMR	103
11	Benzyl trifluoromethyl disulfide	8.3[c]				DNMR	103
12	Benzyl *t*-butyl disulfide	7.8[c]				DNMR	103
13	Benzyl trityl disulfide	8.8[c]				DNMR	103
14	L-Cysteine		23.1	6	17.1	STO-3G	30
15	Diphenyl disulfide		7.5	6.8	0.7	MP2/3-21G*[d]	104
16	bis(1,3,5-tri-i-Pr-Phenyl) disulfide	16.2				DNMR	105

[a] Difference between cis and trans barriers. [b] Geometry optimized at B3LYP/6-31G*. [c] $\Delta G^{\ddagger} = \pm 0.3$ kcal mol^{-1}. [d] Geometry optimized at MP2/3-21G*.

The highest barrier reported, and one of the more interesting results, is that of bis(1,3,5-tri-i-Pr-phenyl) disulfide (entry 16). Kessler and Rundel [105] determined, by low-temperature DNMR, a barrier of 16.2 kcal mol^{-1}, *ca.* 9 kcal mol^{-1} greater than that of **3**. This situation, compared with entry 15, represents an extreme case of steric interactions influencing barrier height. According to the authors, the torsional barriers of less sterically demanding derivatives displayed only C—S bond hindrance.

Although Fraser [103] originally attributed the observed barriers for entries 10–13 to rotation *via* a cis transition state, a conclusion diametrically opposed to the literature, his barrier measurements, coupled with others (*cf.* table 10), clearly indicate that the barrier height does increase with increasing steric bulk [104, 106]. Interestingly, barrier measurements for entry 10 over three solvents (vinyl chloride, CS_2 and toluene) differed little. The authors also reported that barrier height was influenced by the inductive effects of the substituents attached to the S—S bond (*cf.* entries 10 and 11, table 10).

Gas-phase calculations for the barrier of dicubyl disulfide (entry 8) indicate a $S_n \rightarrow \sigma^*_{C\text{–}C}$ interaction leading to a stabilization of the trans transition state and thus, counter-intuitively, to a small decrease in the S—S barrier. In general, gas-phase calculations faithfully reproduced the expected lower trans barrier of *ca.* 6.5 kcal mol^{-1}.

It is therefore possible to influence torsional barriers both stereo-electronically as well as sterically (*vide infra*).

5. Disulfides bearing a halogen next to the S—S bond

Electronegative atoms immediately attached to an S—S bond substantially influence the structural properties of the moiety. The geometries of FSSF (**7a**), BrSSBr (**8a**) and ClSSCl (**9a**) are shown in table 11.

The electron diffraction structures of **7a**–**9a** (entries 1, 7 and 18) show a characteristic decrease in r(S—S), and increases in both the bond and torsional angles for increasing electronegativity of the X substituent. However, this is not the whole story as $(CF_3)_2S_2$ has a normal r(S—S) [118] of *ca.* 2.03 Å even though the inductive effect of the trifluoromethyl group amounts to an electronegativity of 3.7 [119]; similarly, R_2NSSNR_2 has an $\mathbf{r}_{X\text{–}ray}(S\text{—}S) = 2.021$ Å for R = CH_3SO_2 [120]. Cárdenas-Jirón [27] calculated the S—S bond orders for S_2Cl_2 (**9a**) and S_2F_2 (**7a**) to be 1.09 and 1.36, respectively, indicating a substantial degree of double bond character in the latter. Given such a short reported S—S bond for **7a**, it is entirely reasonable that this bond would possess a large degree of double bond character. All three sulfur monohalides possess C_2 symmetry, as with **1a**.

Notably, early electron diffraction work on S_2Cl_2 **9a** contained larger errors with poorly defined structures (these were included for completeness) and entries 7 or 9 should be used as the optimal geometry; the ED data has uncertainties related to electron correlation while the MW data has uncertainties related to zero-point vibrations. Kniep and co-workers [108] are the only ones to report crystal structures of S_2Cl_2 (**9a**) (1.943 Å) and S_2Br_2 (**8a**) (1.970 Å). Their reported structure for **9a** is intermediate between that of the ED and MW data (*cf.* table 11). Interestingly, their r(S—S) for **8a** is much closer to that of **9a** and is shorter by *ca.* 0.03 Å than that determined by Hirota [107].

In general, electron correlation is required to accurately predict the geometric parameters of these dihalodisulfanes. For instance, entry 12 overestimates r(S—S) while entry 14 approaches the experimental geometry with an $r(S\text{—}S) < 2$ Å. Das and Whittenburg [121] have published a high level theoretical study on **9a**. They report that the inclusion of diffuse and d- and f-type polarization functions was necessary to shorten the S—S bond (though they had little effect on increasing the accuracy of the predictions of bond and dihedral angles) and that their inclusion was additive; the MP2 method shows the best agreement among theoretical models [the best basis sets for this method were that of the 6-311+G(2df) and 6-311+G(3df)].

Table 11. Experimental and theoretical structural parameters for dihalodisulfanes.

Entry	X	r(S−S) (Å)	θ(X−S−S) (°)	τ (X−S−S−X) (°)	Method	Ref.[a]
1	Br	1.980 ± 0.040	105.0 ± 3.0	83.5 ± 11.0	ED	107
2	Br	1.948 ± 0.002	109.2 ± 0.1	83.9 ± 0.1	X-ray	108
3	Br	1.964 ± 0.02	107.1 ± 2.9	83.7 ± 0.3	Average [37]	
4	Cl	2.040 ± 0.050	105.0 ± 5.0	90.0	ED	109
5	Cl	2.050 ± 0.030	103.0 ± 2.0		ED	110
6	Cl	1.970 ± 0.030	107.0 ± 2.5	82.5 ± 12.0	ED	107
7	Cl	1.931 ± 0.005	108.2 ± 0.3	84.8 ± 1.3	ED	111
8	Cl		111.0	85.0	CNDO/2	112
9	Cl	1.950 ± 0.001	107.7 ± 0.1	85.2 ± 0.1	MW	113
10	Cl	1.943 ± 0.001	107.1 ± 0.0	84.8 ± 0.1	X-ray	108
11	Cl	2.005	105.9	94.8	HF-SCF/6-31G$*$	27
12	Cl	2.004	105.9	85.1	HF/6-31G*	33
13	Cl	1.979	107.5	85.8	MP2/6-311G**	34
14	Cl	1.976	107.5	85.7	MP2/6-311G(2d,2p)	34
15	Cl	1.985 ± 0.040	106.9 ± 2.0	86.4 ± 3.5	Average [37]	
16	F	1.888 ± 0.010	108.3 ± 0.5	87.9 ± 1.5	MW	114
17	F		110.0	89.0	CNDO/2	112
18	F	1.890 ± 0.002	108.3 ± 0.2	87.7 ± 0.4	ED	115
19	F	1.953	104.2	92.7	HF-SCF/6-31G*	27
20	F	1.953	104.3	88.7	HF/6-31G*	33
21	F	1.953	104.3	88.6	HF/6-31G*	116
22	F	1.923	106.6	88.9	MP2/6-311G**	34
23	F	1.921	108.3	88.6	MP2/6-311G(2d,2p)	34
24	F	1.894	110.4	88.1	X$_\alpha$/DZP	34
25	F	1.952	106.6	88.9	MP2/6-31G*	117
26	F	1.944	105.6	88.9	QCISD/6-31G*	117
27	F	1.910	110.5	89.3	SVWN/6-31G*	117
28	F	1.937	110.6	89.4	BP86/6-31G*	117
29	F	1.942	108.4	89.1	B3LYP/6-31G*	117
30	F	1.928 ± 0.025	107.6 ± 2.4	89.0 ± 1.2	Average [37]	

[a] References are ordered chronologically per section.

For FSSF (**7a**), even with the addition of electron correlation and the inclusion of larger basis sets as in entry 23, there still is no convergence in the geometry; r(S−S) is overestimated by *ca.* 2%. In fact, DFT methods [117, 122] (entries 24 and 27) provide much more accurate predictive methods. As can be seen, modeling these electronically related systems to the dialkoxy disulfides (*vide infra*) is non-trivial.

To date, the barriers to rotation of halosulfanes have not been experimentally determined. Some workers have calculated their barriers and the results are shown in table 12.

The addition of one halogen atom increases the cis barrier by *ca.* 3–5 kcal mol^{-1} over that of **1a**. The effect is multiplicative when two halogens are attached, with an increase of *ca.* 10–17 kcal mol^{-1} depending on the nature of the halogen. Barrier calculations performed using the HF method should be taken with a degree of caution as this method is poor when it comes to predicting barrier height (*vide supra*). Nevertheless, the calculations do indicate that the S−S barrier is sensitive to the nature of the attached substituents; the sensitivity and barrier magnitudes here are much greater than those of the XOOX analogs [33].

Table 12. Calculated barriers to rotation for some halodisulfane and dihalodisulfanes.

Compd		Calculated (kcal mol^{-1}) cis	trans	Δ^{a} (kcal mol^{-1})	Method	Ref
HSSCl	**10**	10.7			HF/6-31+G*	27
ClSSCl	**9a**	17.0			HF/6-31+G*	27
		17.1	11.9	5.2	HF/6-31G*	33
		20.2	15.4	4.8	MP2/6-311+G(3df)	121
HSSF	**11**	12.8			HF/6-31+G*	27
FSSF	**7a**	25.3			HF/6-31+G*	27
		24.2	18.9	5.2	HF/6-31G*	33

[a] Difference between cis and trans barriers.

The high barrier calculated for FSSF (**7a**) coupled with the short r(S−S) has been attributed to two hyperconjugative interactions between the 3p lone pairs of each sulfur which are partially delocalized into the adjacent σ^*_{S-F} antibonding orbitals. This delocalization is maximized given a *gauche* conformation. MO overlap is maximized as the energy of the σ^* orbital is lowered, so we would expect that the more electronegative the atom the higher the barrier (figure 3b). This interaction exists in HSSH (**1a**), ClSSCl (**9a**), HOOH (**2a**) as well as FOOF (**12**) and has previously been discussed [123, 124].

6. Dialkoxy disulfides

Highly chalcogenated dialkoxy disulfides (ROSSOR) possess many structural features that are similar to those observed for FSSF (**7a**). Even with vastly different substituents, all dialkoxy disulfides possess many structurally similar features as outlined in table 13.

Although Steudel and co-workers [125] originally used the HF/6-311G** method to model the geometry of HOSSOH (**13a**), we [131] have subsequently shown that this method is inadequate for accurately modeling this class of compounds. Rather, MP2 perturbation theory or DFT methods such as SVWN, B3PW91 or B3P86 with a sufficiently large basis set (minimum 2 d-type polarization functions included in the basis set) were required to converge the geometry.

As with all other XSSX systems, the preferred conformation of dialkoxy disulfides is one that allows for the maximum orbital overlap between each sulfur lone pair and its adjacent

Table 13. Experimental and theoretical structural parameters for acyclic dialkoxy disulfides.

Entry	R	r (S−S)	r_{av} (O−S)	θ_{av} (O−S−S)	τ (O−S−S−O)	Method	Ref.[a]
1	H	2.013	1.647	105.1	85.7	HF/ 6-311G**	125
2	Me	1.972 ± 0.001	1.658 ± 0.004	108.2 ± 0.1	81.5 ± 0.1	X-Ray	126
3	Me	1.960 ± 0.003	1.653 ± 0.003	108.2 ± 0.3	91 ± 4	ED	127
4	p-NO$_2$-Bn	1.958 ± 0.001	1.653 ± 0.003	107.7 ± 0.1	85.5 ± 0.1	X-Ray	128
5	p-Cl-Bn	1.932 ± 0.003	1.644 ± 0.009	108.9 ± 0.3	76.8 ± 0.5	X-Ray	129
6	4-I-cubyl-methyl	1.970 ± 0.003	1.645 ± 0.006	107.8 ± 0.3	87.6 ± 0.3	X-Ray	130

[a] References ordered chronologically.

S−O antibonding orbital. The presence of the oxygen atom substantially lowers the energy of the antibonding orbital, resulting in an S−S bond with significant double bond character. This is a manifestation of a generalized anomeric effect, which substantially increases the S−S rotational barrier to *ca.* 19 kcal mol^{-1} [128, 132, 133].

7. Isomerization of S−S bond to a branched species

An important feature of the work reviewed here revolves around the stability and mechanism of isomerization of divalent disulfide isomer **14a** to thiosulfoxide-like isomer **14b** (scheme 1). The S−S bond in **14b** may either be considered as having double bond [134] character or containing a single semipolar [135] bond depending on the electronegativity of the substituent X. The double bond character in **14a** is also influenced by the inductive nature of X (*vide supra*).

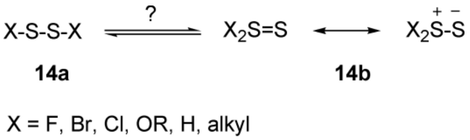

SCHEME 1

8. General commentary on X−S−S−X/X$_2$S=S systems

The concept of the existence of branch-bonded S−S species has generated considerable debate and investigation [136]. Foss first popularized the notion that branch-bonded sulfur molecules of the form **14b** bonded *via* $S_{3d}-S_p$ orbital interactions and that these were only stabilized when the branched sulfur was attached to an electronegative group [136, 137]. The following sections overview related isomerization reactions involving sulfur, and the respective stabilities of each isomer are highlighted.

9. R−S−S−R/R$_2$S=S systems

To date [138], no organic polysulfide **14b** has been isolated in the solid or liquid phase that contains a branched, thiosulfoxide arrangement ($R_2S=S$, R = alkyl or H). The concept of hypervalent sulfur species was first introduced by Foss [137] although reports of the existence of thiosulfoxides date from the early 20th century, most specifically dealing with the distillation of Levinstein H (mustard gas) [139]. The controversy surrounding the existence of thiosulfoxides both as reactive intermediates and as stable entities has not abated.

Recently [140] it has been shown *via* tandem mass spectrometry that, in the gas phase, thiosulfoxides are stable entities both as radical cations as well as neutral species ($R_2S=S$, R=H, CH_3, C_2H_5). Steudel provided evidence by IR (bands *ca.* 670 cm^{-1}) more than 30 years ago that branched-sulfur arrangements (−S−S(=S)−S−) could exist in sulfur homocycles at below −150 °C [141, 142]. Calculations at the MP2/6-31G* level of theory now demonstrate that although the unbranched disulfide connectivity is more stable, that of the thiosulfoxide represents a local minimum [35]. Another study showed that although HSSH is the global minimum by *ca.* 38 kcal mol^{-1} in the isomerization of HSSH (**1a**) ⇎ $H_2S=S$(**1b**), nevertheless (**1b**) was also found as a true local minimum on the potential energy surface [19]. Schleyer and co-workers [143], in a comprehensive theoretical study, showed that the energy stabilization for XSSX (**14a**; X=H **1a**, CH_3 **3a**) with respect to the branched isomer is large (averaging 33 and 19 kcal mol^{-1} respectively for **1a** and **3a**) and proportional to the S−S bond length. Bonding of hypervalent and non-hypervalent species of this type are similar and do not involve any special S-3d orbitals according to natural population analysis. The hypervalent-like structure of **14b** is better characterized as a polarized σ-bond (the terminal sulfur being negatively charged) with its strength depending on the electrostatic interactions and the origin of the X group [116].

Steudel and co-workers showed, *via ab initio* calculations, that thiosulfoxides **14b** (R=H, CH_3) should be both kinetically and thermally stable at low temperatures. However, they determined that the unimolecular isomerization barrier to the more stable disulfides (MeSSMe is calculated to be *ca.* 20 kcal mol^{-1} more stable than $Me_2S{=}S$ whereas HSSH **1a** is calculated to be *ca.* 34 kcal mol^{-1} more stable than $H_2S{=}S$, **1b**) would be energetically unfavorable (*ca.* 81 and 52 kcal mol^{-1} respectively for Me and H for an X_2S_2 system) and that at low temperature they should exist as discrete entities [35]. These studies corroborate previous theoretical [112, 116] and experimental [12, 58, 112, 144–146] studies. A corollary to this is that at lower temperatures ($<100\,°C$) thiosulfoxides cannot be invoked as intermediates in interconversion reactions involving polysulfides.

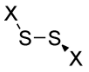

14a

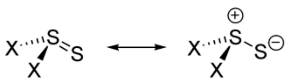

14b

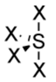

15

Notably, Steudel [147] recently probed the formation of sulfuranes **15** as possible hypervalent intermediates in the interconversion of sulfur allotropes and of chain-like polysulfides at moderate temperatures and found these species to be too energetically disfavored; the formation of thiosulfoxides as intermediates at similar temperatures had previously been investigated and also found to be energetically disfavored [32]. It was therefore concluded that such reactions proceed through a radical dissociation mechanism at higher temperatures and are initiated at more moderate temperatures by either trace nucleophile impurities in solution or by polar groups present on the reaction vessel which themselves may serve as catalysts.

Prior to the mass spectrometry study by Gerbaux [140] and co-workers, the existence of thiosulfoxides had only been inferred. It has been proposed that thiosulfoxides are intermediates in the eventual deoxygenation of sulfoxides with thiophosphoryl bromide ($PSBr_3$) [148] or phosphorus pentasulfide (P_4S_{10}) [149–151] (scheme 2a-probably proceeding in a similar manner to the oxaphosphetane formed during the Wittig reaction), as well as in the sulfurization then isomerization of allylic sulfoxides (*via* a [2,3]-sigmatropic shift) to the corresponding disulfide using B_2S_3 (scheme 2b) [152–154]. Thiosulfoxide intermediates have also been posited in the formation of sulfides from the reaction of sulfilimines ($R_2S{=}N{-}X$; X=H, Tos) or sulfur ylids with P_4S_{10} in work by Oae [155, 156] and Still [157]. Phosphorus pentasulfide (P_4S_{10}) in particular has been synthetically useful. Illustrative examples include its use, in the presence of pyridine, to deoxygenate penicillin (**16**) and cephalosporin (**17**) sulfoxides [158] as well as allenyl sulfoxides [159].

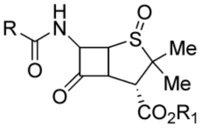

penicillin
sulfoxide

16

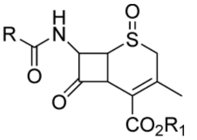

cephalosporin
sulfoxide

17

The existence of an undetectably small equilibrium between allylic disulfides and their thiosulfoxide isomers was proposed by Mislow and co-workers [160] over 30 years ago to account for the formation of allyl disulfides from the reaction of allyl sulfides with sulfur (scheme 3a) or the sigmatropic rearrangement of allyl disulfides (scheme 3b) [161]. Desulfurization of allyl

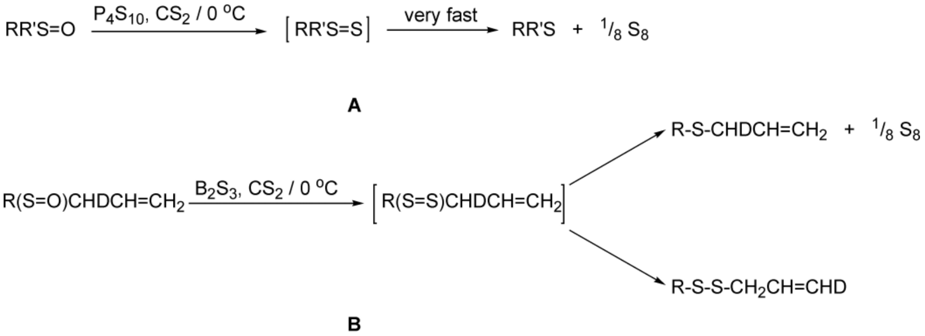

SCHEME 2 Generation of thiosulfoxides as intermediates.

disulfides with Ph_3P below 100 °C was also proposed to proceed *via* a thiosulfoxide intermediate [162]; saturated disulfides did not desulfurize under these conditions [163]. Others have also implied the formation of thiosulfoxides although they too were unable to detect them [151, 164]. Steudel [35] has calculated that even though MeSSAllyl is more stable than MeAllylS=S, by *ca.* 20 kcal mol^{-1}, its isomerization only requires ca. 26 kcal mol^{-1}, much less than that calculated for saturated disulfides (*vide supra*).

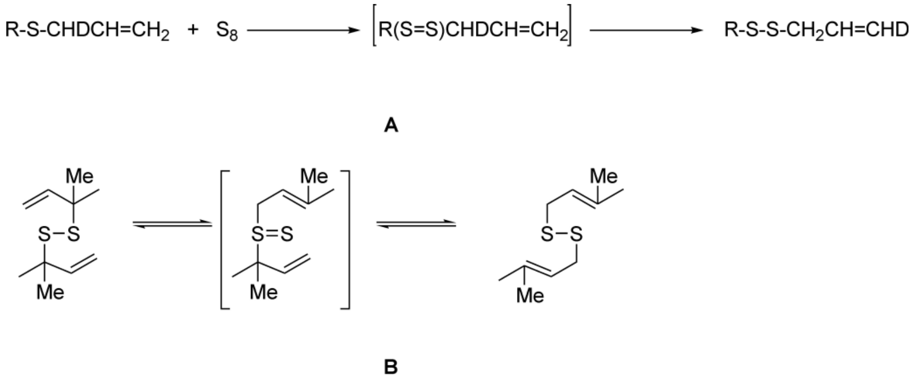

SCHEME 3 Thiosulfoxides as intermediates in isomerization reactions.

Thiosulfoxides have been proposed as intermediates in photolytic [165] (scheme 4a) and thermolytic [134, 166] (scheme 4b) desulfurization reactions.

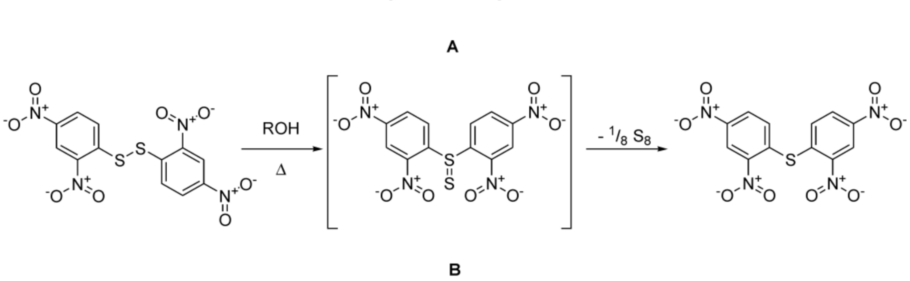

SCHEME 4 Thiosulfoxides as intermediates in thermal and photochemical reactions.

Thiosulfoxides have also been postulated as intermediates in the efficient reduction of sulfoxides with TFAA$-$$H_2S$ ($>$90%, 5 min) [167] or hexamethyldisilathiane [168], $[(Me)_3Si]_2S$, to the corresponding sulfide; in the latter case, the increased strength of the Si$-$O over the Si$-$S bond (*ca.* 106 and 70 kcal mol^{-1}, respectively) provides the driving force for the reaction.

An explanation of the work to date suggests that the heats of formation of thiosulfoxides and branched sulfur species in the interconversion of sulfur homocycles [169] lie as little as *ca.* 10 kcal mol^{-1} above the unbranched disulfides [134, 170].

Little work has been done on the isomerization of higher order polysulfides to their respective branch-bonded isomers. Barnard and co-workers [171] have proposed a branch-bonded trisulfide as an intermediate in the thermal racemization of bis(1,3-dimethylbut-2-enyl) trisulfide. Safe and Taylor [172] were proponents of an equilibrium between branched and unbranched trisulfides as an explanation of the conversion of disulfides into trisulfides by reaction with H_2S_2 (**1**). Recently, the ground-state energy difference between H_2S_6 and $(HSS)_2S{=}S$ has been calculated at a high level of theory [G3X-(MP2)] to be only *ca.* 13 kcal mol^{-1} at 0 K [173]. However, to date no evidence exists for branched isomers of polysulfides ($n > 2$).

Branch-bonded $X_2S{=}S$ structures have been detected and are considered stable entities when X is electronegative; the physical properties of these compounds (where X = F, O, Cl, Br) is covered in the following sections.

10. F-S–S-F/$F_2S{=}S$ system

As will be seen, isomer **14a** (with C_2 symmetry) is the most common. In some special cases, the thiosulfoxide isomer **14b** (with C_s symmetry) has also been detected. Historically, the first isolation and identification (via IR, MW and MS) of each of the valence-bond isomers in scheme 1 was that of the sulfur monofluoride (S_2F_2) system. Kuczkowski's [114, 174, 175] seminal work has since been experimentally [115, 176–184] and theoretically [28, 34, 112, 115–117] confirmed by others. The unbranched isomer FSSF (**7a**) was initially regarded [179] as the less stable isomer as it was reported to isomerize to the branch-bonded F_2S_2 (**7b**) at temperatures above -100 °C [176, 178, 179]. To complicate the analysis, Seel and Budenz postulated that **7b** in the gas phase is transformed into the complex [FSSF, F_2S_2](g) upon cooling the sample to -80 °C [176]. This would seem to indicate that, at lower temperatures, **7a** is the most stable isomer. These two observations would seem to be initially at odds, yet nevertheless demonstrate that the isomers **7a** and **7b** are of comparable ground-state energies. The physical properties of **7a** and **7b** are outlined in Table 14.

Table 14. Physical properties of sulfur monofluoride **7**.

Compd[a]	Connectivity	Mp (°C)	Bp (°C)
7a	F$-$S$-$S$-$F	-133[b]	15[b]
7b	$F_2S{=}S$	-164.6[c]	-10.6[c]

[a] Each isomer is a colorless gas at room temperature. [b] From ref. [178]. [c] From ref. [183].

Brown and Pez [178] were the first to investigate the isomerization of **7a** to **7b**. They noted that Lewis acids such as HF or BF_3 catalyzed the conversion of liquid **7a** into **7b** and postulated a possible mechanism (scheme 5).

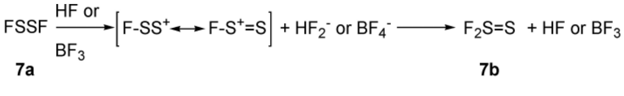

$$\underset{\mathbf{7a}}{\mathrm{FSSF}} \xrightarrow[\mathrm{BF_3}]{\mathrm{HF\ or}} \left[\mathrm{F{-}SS^+} \longleftrightarrow \mathrm{F{-}S^+{=}S}\right] + \mathrm{HF_2^-\ or\ BF_4^-} \longrightarrow \underset{\mathbf{7b}}{\mathrm{F_2S{=}S}} + \mathrm{HF\ or\ BF_3}$$

SCHEME 5

Under the same conditions, **7b** decomposes into S_8 and SF_4; thiothionyl fluoride (**7b**) is a stable gas up to at least 400 °C in the absence of a Lewis acid. Their preliminary kinetics measurements indicated that the Lewis acid promoted isomerization was first order and that **7b** was the more stable isomer at room temperature (21.8 ± 0.3 °C) [178]; **7a** had a $t_{1/2} = 4.7\,\mathrm{h}$. They did, however, determine that **7a** was the more stable isomer at −50 °C over CsF, in general agreement with Seel's observation [176]. CsF seems to stabilize **7a** relative to **7b**. Lösking [185] reported that the **7b** is more stable by $2.7 \pm 0.4\,\mathrm{kcal\,mol^{-1}}$.

Cao [184, 186] and co-workers have reported the PES spectra of **7a** and **7b** as well as the isomerization between the two. They determined that **7a** is the more stable isomer *above* −80 °C and determined that the kinetics of isomerization of **7b** to **7a** are first order ($k_{296\mathrm{K}} = 3.8 \pm 0.4 \times 10^{-5}\,\mathrm{s^{-1}}$) with an activation barrier E_A for the forward direction of $5.8\,\mathrm{kcal\,mol^{-1}}$. This observed reversal of stability as compared with that of the literature should be viewed with caution.

Several groups have probed the isomerization of sulfur monofluoride **7** computationally. Solouki and Bock [112] investigated the isomerization in scheme 1 by semi-empirical methods (CNDO/2). They determined that as the electronegativity of X increases, the thiosulfoxide isomer **14b** becomes more stabilized. Solouki and Bock proposed that there exists a substantial isomerization barrier between **7a** and **7b** of 23–46 $\mathrm{kcal\,mol^{-1}}$ [187].

More recently, Bickelhaupt and co-workers [34] explored the relative energies of **7a** and **7b** and related systems. They corroborated the earlier work [112] that stated that the ground-state energy difference between **14a** and **14b** decreases as the electronegativity of X increases. They determined that the energy difference for **7a** and **7b** was small and dependent on the level of *ab initio* theory used. For instance, at QCISD(T)/6-31G**//MP2/6-31G** **7b** is the more stable by $0.3\,\mathrm{kcal\,mol^{-1}}$ whereas at QCISD(T)/6-31+G**//MP2/6-31G** **7a** is the more stable by $3\,\mathrm{kcal\,mol^{-1}}$. Such a range in energies is due to the polarized nature of **7b** wherein both the terminal sulfur and the fluorines acquire a substantial negative charge. Diffuse and polarization functions were thus required to accurately describe such compounds although these had a net neutralizing effect on the overall energy difference (total stabilization effect is $1.7\,\mathrm{kcal\,mol^{-1}}$ for **7a**). This confirmed the early *ab initio* work of Marsden [115] and co-workers, though at the time Marsden believed that **7b** was the more stable isomer and had difficulty rectifying this with his theoretical results (this apparent conflict can be explained *vide infra*). Jursic [122] has published a comprehensive DFT study wherein geometries converged (B3P86 was the best method) but energies predicted the wrong isomer **7a** as the more stable; he conjectured that using the MP2 method would yield better energies. The relative ground state energies for S_2X_2 systems are summarized in table 15.

In investigating the mechanism for the rearrangement between **7a** and **7b**, Bickelhaupt and co-workers [34] confirmed the earlier barrier calculations assuming that the isomerization proceeds *via* a 1,2-F shift in a unimolecular mechanism (40.7–51.5 $\mathrm{kcal\,mol^{-1}}$ depending on level of theory, ZPE correction included). The addition of electron correlation and diffuse functions reduced this barrier substantially yet the barrier still remains high. DFT (NL BP86) energies [117] of the same barrier are corroborative.

Such calculated barriers are disconnected from the experimental observations of an equilibrium between the two isomers at low temperatures (−100 °C) [176, 179]. This inconsistency implies that the pathway is not unimolecular (as had been originally proposed by Bock and Solouki, involving a 1,2-F shift *via* a three-membered ring transition state – **TS 2**) and the authors [34] have suggested a bimolecular mechanism with possible transition states as outlined in scheme 6 (**TS 1**).

Careful attention must be taken when interpreting theoretical energies as these are usually calculated without any consideration of temperature. Torrent and co-workers [117] have calculated the respective energies of **7a** and **7b** with ZPVE and thermal corrections and determined that, at room temperature, **7b** is the more stable isomer whereas at low temperatures **7a**

Table 15. Relative energies of S_2X_2 (**14b**) with respect to XSSX (**14a**) isomers [34].

X	EN[a]	QCISD(T)/6-31G**//MP2/6-31G** XSSX (Hartrees)	S_2X_2 (Hartrees)	△[b] (kcal mol^{-1})	QCISD(T)/6-31+G**//MP2/6-31G** XSSX (Hartrees)	S_2X_2 (Hartrees)	△[b] (kcal mol^{-1})	△△[c] (kcal mol^{-1})
F	4.1	−994.46225	−994.46273	−0.3	−994.50082	−994.49610	3.0	3.3
Cl	2.8	−1714.51823	−1714.49275	16.0	−1714.52799	−1714.50400	15.1	−0.9
H	2.5	−796.47540	−796.42237	33.3	−796.47907	−796.42663	32.9	−0.4
Me	2.2	−874.82574	−874.79478	19.4	−874.83390	−874.80481	18.3	−1.2

[a] Allred-Rochow electronegativities, ref. [188]. [b] Energy difference between two isomeric forms; a '−' sign signifies that S_2X_2 is more stable. [c] Energy difference relative to the inclusion of diffuse functions.

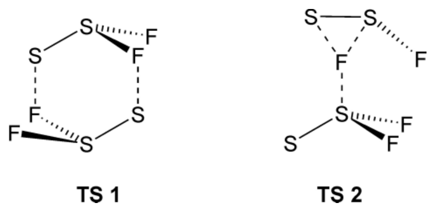

SCHEME 6 Possible bimolecular transition states in the isomerization of **7**.

is the more stable isomer. The low temperature activation parameters agree well with earlier work reported by Marsden [115] and Bickelhaupt [34] as well as that observed experimentally (though Marsden did not acknowledge the thermal dependence on the relative stability of isomers **7a** and **7b**).

To summarize, disulfane **7a** appears to be the more stable isomer at low temperatures (*ca.* −100 °C) whereas branch-bonded **7b** is the more stable isomer at higher temperatures (−80 to 400 °C). To date, no plausible mechanism for this isomerization has been proposed based on experimental findings though the calculated 1,2-F shift reported by some possesses a barrier that is too large to account for the observed low temperature isomerization.

11. Cl-S–S–Cl/Cl_2S=S and Br-S–S–Br/Br_2S=S systems

Relative to S_2F_2, much less work exists in the literature on the relative stabilities of isomeric forms of sulfur monochloride (**9a**) and sulfur monobromide (**8a**) despite the considerable utility of **9a** as a reagent in organic chemistry. Though thiothionyl chloride (**9b**) has been suggested as a minor equilibrium contributor by some [189–191], the ED [107, 109–111], Raman [192–196], IR [194], PES [197], dipole moment [198], quasi-elastic neutron scattering [199] and MW [113] studies all suggest that S_2Cl_2 exits in one isomeric form as **9a**. Chadwick and co-workers [200] and Feuerhahn and Vahl [201] both reported the presence of low concentrations of **9b**, once **9a** deposited in argon matrices at low temperature (8–20 K) had been UV photolyzed. These last two reports should be taken as artifacts of the observation technique.

Bock and Solouki [112] calculated that the most stable isomer was that of the unbranched **9a** and that the interconversion barrier was only *ca.* 3.5 kcal mol^{-1} based on the CNDO/2 hyperenergy surface. However, Das [202] at a high level of theory (QCISD/6-311+G(3df)//QCISD/6-311G(3d)) determined the barrier at 0 K to be *ca.* 51 kcal mol^{-1}; the latter case presumes a unimolecular mechanism involving a 1,2-Cl shift with a 3-membered ring transition state, similar to that reported for the S_2F_2 system (*vide supra*). Similar to the S_2F_2 system, Bickelhaupt [34] calculated the relative ground state energies of **9a** and **9b**. At the QCISD(T)/6-31G**//MP2/6-31G** level **9a** is more stable by *ca.* 16.0 kcal mol^{-1}, while adding diffuse functions in QCISD(T)/6-31+G**//MP2/6-31G** destabilized **9a** slightly relative to **9b** (15.1 kcal mol^{-1}). In general, the addition of diffuse functions destabilized the XSSX isomer but not significantly so. A higher barrier than that calculated by Bock would be expected given the lack of experimental evidence for the existence of the branched structure.

The little work carried out on the isomerization of S_2Br_2 **8** suggests that it too exists in its unbranched form [107, 194, 196, 199] though, as with S_2Cl_2, Feuerhahn and Vahl [201] claim to have observed thiothionyl bromide (**8b**).

12. Commentary on the RO–S–S–OR/$(RO)_2S$=S System (R = H, R′)

Steudel and co-workers have investigated the isomerization between dialkoxy disulfides (ROSSOR) and thionosulfites (ROS(S)OR). The transient preparation of dihydroxy disulfide HOSSOH (**13a**), the unbranched form of thiosulfurous acid, has been reported [203, 204];

although no information about its physical properties exist it has been observed in the EI mass spectrometry of parent ROSSOR compounds (R = alkyl), which are themselves known to exist [126, 130, 132, 205–209].

There are at least 11 isomeric structures of HOSSOH (**13**) and their geometries and energies have been calculated. The four lowest energy isomers are shown in table 16 [125].

Table 16. Calculated [125] relative energies (kcal mol^{-1}) of the four most stable isomers of HOSSOH (**13**).

	HO−S−S−OH **13a**	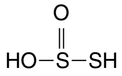 $HO-\overset{O}{\overset{\|}{S}}-SH$ **13b**	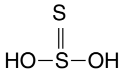 $HO-\overset{S}{\overset{\|}{S}}-OH$ **13c**	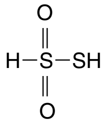 $H-\underset{O}{\underset{\|}{\overset{O}{\overset{\|}{S}}}}-SH$ **13d**
MP4/6-31G*//HF/6-31G*	0	3.2	3.9	23.5

The relative energy differences of the first three structures (**13a–c**) are small as compared with the fourth, **13d**. When the energies of these three structures are further refined using larger basis sets (MP2/6-311G**//HF/6-311G** + ZPVE), their relative energy differences decrease (**13a** = 0, **13b** = −0.3, **13c** = 3.2 kcal mol^{-1}); **13b** has not been experimentally detected. The related tetrasulfide HSSSSH (**18a**) is 33.0 kcal mol^{-1} more stable than its branch-bonded analog $(HS)_2S{=}S$ **18b** [115], whereas the branch-bonded S_2F_2 (**7b**) is the more stable isomer in that system (*vide supra*) [210]. Thus, the inclusion of electronegative atoms such as oxygen stabilizes the branch bonded form **13b** over the unbranched **13a**.

Acyclic esters of dihydroxy disulfide can be easily prepared. There exists four structurally resolved acyclic dialkoxy disulfides ROSSOR (R = Me [126, 127, 209], *p*-NO_2-Bn [133, 207], *p*-Cl-Bn [129], 4-iodocubylmethyl [130]). Thionosulfites containing a 5-membered ring core can also be prepared [211–213]. Recently, we probed the origin of the isomeric stability in this class of compounds and concluded, from a combined theoretical and experimental study, that dialkoxy disulfides are the more stable isomeric forms when the compounds possess a sufficiently large (8 atoms or larger) chalcogenated ring. Below this threshold, thionosulfites appear more stable. Moreover, the energy difference between the two isomeric forms is proportional to the number of atoms in the heterocyclic ring. The decrease in stability of dialkoxy disulfides relative to thionosulfites appears to be due to the presence of their significantly distorted O−S−S−O dihedral angle that would be necessary to accommodate the ring [208].

Acknowledgments

We thank NSERC and FQRNT (formerly FCAR) for funding. EZ-C acknowledges support from FQRNT in the form of a postgraduate scholarship. We thank J. P. Snyder (Emory University) for helpful contributions.

References

[1] Langs, D. A., Smith, G. D., Stezowski, J. J. and Hughes, R. E., 1986, *Science*, **232**, 1240–1242.

[2] The structure of oxytocin is Cys^1-Tyr^2-Ile^3-Gln^4-Asn^5-Cys^6-Pro^7-Leu^8-Gly^9-NH_2, containing a disulfide bridge between the two cysteine amino acids forming a hexapeptide ring. The structure of vasopressin differs in two positions: Phe^3 and Arg^8. Both are neurohypophyseal hormones.

[3] Garrett, R. H. and Grisham, C. M., 1995, Biochemistry (2nd edn) (New York: Saunders College Publishing), pp. 189–191.

[4] H–H BDE = 104 kcal mol^{-1}; C–C BDE = 79 kcal mol^{-1}.
[5] Oae, S., 1996, *Main Group Chem. News*, **4**, 10–17.
[6] Poisel, H. and Schmidt, U., 1971, *Angew. Chem. Int. Ed. Engl.*, **10**, 130–131.
[7] Hald, J., Jacobsen, E. and Larsen, V., 1948, *Acta Pharmacol. Toxicol.*, **4**, 285–296.
[8] Nieuwenhuizen, P. J., Ehlera, A. W., Hofstraat, J. W., Janse, S. R., Nielsen, M. W. F., Reedijk, J. and Barends, E. J., 1998, *Eur. J. Chem.*, **4**, 1816–1821.
[9] Kato, S., Hamada, Y. and Shiroji, T., 1986, *Tetrahedron Lett.*, **27**, 2653–2656.
[10] Menger, F. M. and Caran, K. L., 2000, *J. Am. Chem. Soc.*, **122**, 11679–11691.
[11] Winnewisser, G. and Haase, J., 1968, *Z. Naturforsch. A*, **23**, 56–60.
[12] Winnewisser, G., Winnewisser, M. and Gordy, W., 1968, *J. Chem. Phys.*, **49**, 3465–3478.
[13] Winnewisser, G., 1972, *J. Mol. Spectrosc.*, **41**, 534–547.
[14] Redington, R. L., 1962, *J. Mol. Spectrosc.*, **9**, 469–476.
[15] Aida, M. and Nagata, C., 1986, *Theor. Chim. Acta*, **70**, 73–80.
[16] Winnewisser, G., 1972, *J. Chem. Phys.*, **56**, 2944–2954.
[17] Winnewisser, G. and Helminger, P., 1972, *J. Chem. Phys.*, **56**, 2967–2979.
[18] Hahn, J., Schmidt, P., Reinartz, K., Behrend, J., Winnewisser, G. and Yamada, K. M. T., 1991, *Z. Naturforsch. B*, **46**, 1338–1342.
[19] Marsden, C. J. and Smith, B. J., 1988, *J. Phys. Chem.*, **92**, 347–353.
[20] Harmony, M. D., Laurie, V. W., Kuczkowski, R. L., Schwendeman, R. H., Ramsay, D. A., Lovas, F. J., Lafferty, W. J. and Maki, A. G., 1979, *J. Phys. Chem. Ref. Data*, **8**, 619–621.
[21] Herbst, E. and Winnewisser, G., 1989, *Chem. Phys. Lett.*, **155**, 572–575.
[22] Allen, H. C. and Plyler, E. K., 1956, *J. Chem. Phys.*, **25**, 1132–1136.
[23] Ha, T.-K., Nguyen, M. T. and Vanquickenborne, L. G., 1982, *J. Mol. Struct. (THEOCHEM)*, **7**, 107–114.
[24] Ha, T.-K., Nguyen, M. T. and Vanquickenborne, L. G., 1982, *J. Mol. Struct. (THEOCHEM)*, **7**, 99–105.
[25] Cremer, D., 1978, *J. Chem. Phys.*, **69**, 4440–4455.
[26] Bair, R. A. and Goddard III, W. A., 1982, *J. Am. Chem. Soc.*, **104**, 2719–2724.
[27] Cárdenas-Jirón, G. I., Cárdenas-Lailhacar, C. and Toro-Labbé, A., 1993, *J. Mol. Struct. (THEOCHEM)*, **282**, 113–122.
[28] Hinchliffe, A., 1979, *J. Mol. Struct.*, **55**, 127–134.
[29] Ha, T.-K., 1985, *J. Mol. Struct. (THEOCHEM)*, **122**, 225–234.
[30] Boyd, R. J., Perkyns, J. S. and Ramani, R., 1983, *Can. J. Chem.*, **61**, 1082–1085.
[31] Dixon, D. A., Zeroka, D., Wendoloski, J. J. and Wasserman, Z. R., 1985, *J. Phys. Chem.*, **89**, 5334–5336.
[32] Steudel, R., Laitinen, R. S. and Pakkanen, T. A., 1987, *J. Am. Chem. Soc.*, **109**, 710–714.
[33] Samdal, S., Mastryukov, V. S. and Boggs, J. E., 1994, *J. Mol. Struct. (THEOCHEM)*, **309**, 21–31.
[34] Bickelhaupt, F. M., Solà, M. and Schleyer, P. v. R., 1995, *J. Comput. Chem.*, **16**, 465–477.
[35] Steudel, R., Drozdova, Y., Miaskiewicz, K., Hertwig, R. H. and Koch, W., 1997, *J. Am. Chem. Soc.*, **119**, 1900–1996.
[36] Koput, J., 1996, *Chem. Phys. Lett.*, **259**, 146–150.
[37] The average structural parameters represent a virtual structure and are placed solely for the reader's convenience.
[38] Fleming, I., 1976, Frontier orbitals and organic chemical reactions (London: John Wiley & Sons).
[39] Mulliken, R. S., 1955, *J. Chem. Phys.*, **23**, 1833–1840.
[40] Boyd, D. B., 1972, *J. Am. Chem. Soc.*, **94**, 8799–8804.
[41] Steudel, R., 1982, *Top. Curr. Chem.*, **102**, 149–176.
[42] Freed, K., 1968, *Chem. Phys. Lett.*, **2**, 255–256.
[43] Laitinen, R. and Pakkanen, T., 1985, *J. Mol. Struct. (THEOCHEM)*, **124**, 293–305.
[44] Veillard, A. and Demuynck, J., 1970, *Chem. Phys. Lett.*, **4**, 476–478.
[45] Rauk, A., 1984, *J. Am. Chem. Soc.*, **106**, 6517–6524.
[46] Lowe, J. P., 1970, *J. Am. Chem. Soc.*, **92**, 3799–3800.
[47] Schleyer, P. v. R., Kaupp, M., Hampel, F., Bremer, M. and Mislow, K., 1992, *J. Am. Chem. Soc.*, **114**, 6791–6797.
[48] Pophristic, V. and Goodman, L., 2001, *Nature*, **411**, 565–568.
[49] Schreiner, P. R., 2002, *Angew. Chem. Int. Ed. Engl.*, **41**, 3579–3581.
[50] The most stabilizing hyperconjugative interaction occurs in the ground state (n_S to σ^*_{S-H}) *vide supra*.
[51] Lowe, J. P., 1969, *J. Chem. Phys.*, **51**, 832–836.
[52] Veillard, A., 1969, *Chem. Phys. Lett.*, **4**, 51–52.

[53] The potential energy function $V(\tau)$ can be expanded as a trigonometric series of the form $V(\tau) = V_1\cos(\tau) + V_2\cos 2\tau + V_3\cos 3\tau + \ldots$ where V_n represents the n-fold torsional component. See: Koput, J., 1996, *Chem. Phys. Lett.*, **259**, 146–150.

[54] Hunt, R. H., Leacock, R. A., Peters, C. W. and Hecht, K. T., 1965, *J. Chem. Phys.*, **42**, 1931–1946.

[55] Smyth, C. P., Lewis, G. L., Grossman, A. J. and Jennings III, F. B., 1940, *J. Am. Chem. Soc.*, **62**, 1219–1223.

[56] Sutter, D., Dreizler, H. and Rudolph, H. D., 1965, *Z. Naturforsch. A*, **20**, 1676–1681.

[57] Beagley, B. and McAloon, K. T., 1971, *Trans. Faraday Soc.*, **67**, 3216–3222.

[58] Yokozeki, A. and Bauer, S. H., 1976, *J. Phys. Chem.*, **80**, 618–625.

[59] Van Wart, H. E., Shipman, L. L. and Scheraga, H. A., 1974, *J. Phys. Chem.*, **78**, 1848–1853.

[60] Allinger, N. L., Hickey, M. J. and Kao, J., 1976, *J. Am. Chem. Soc.*, **98**, 2741–2745.

[61] Donohue, J., Caron, A. and Elihu, G., 1961, *J. Am. Chem. Soc.*, **83**, 3748–3751.

[62] Abrahams, S. C., 1955, *Acta Crystallogr.*, **8**, 661–671.

[63] Scott, D. W., Finke, H. L., Gross, M. E., Guthrie, G. B. and Huffman, H. M., 1950, *J. Am. Chem. Soc.*, **72**, 2424–2430.

[64] Hubbard, W. N., Douslin, D. R., McCullough, J. P., Scott, D. W., Todd, S. S., Messerly, J. F., Hossenlopp, I. A., George, A. and Waddington, G., 1958, *J. Am. Chem. Soc.*, **80**, 3547–3554.

[65] El-Sabban, M. Z. and Scott, D. W., 1970, *U.S. Bur. Mines Bull.*, **654**.

[66] Senning, A., 1971, Sulfur in organic and inorganic chemistry (New York: M. Dekker).

[67] Perahia, D. and Pullman, B., 1971, *Biochem. Biophys. Res. Commun.*, **43**, 65–68.

[68] Yamabe, H., Kato, H. and Yonezawa, T., 1971, *Bull. Chem. Soc. Jpn.*, **44**, 604–610.

[69] Jiao, D., Barfield, M., Combariza, J. E. and Hruby, V. J., 1992, *J. Am. Chem. Soc.*, **114**, 3639–3643.

[70] Reinhardt, L. A., 1994, The radical cation chain oxygenation of olefins and dienes, the physical properties of olefins and dienes and their radical cations, and the conformational analysis of polyoxysulfides. PhD. thesis, Madison: University of Wisconsin-Madison.

[71] The V_1 term is associated with dipole-dipole interactions. V_2 is associated with hyperconjugation. V_3 is associated with steric repulsion.

[72] Radom, L., Hehre, W. J. and Pople, J. A., 1972, *J. Am. Chem. Soc.*, **94**, 2371–2381.

[73] For an extensive survey of structural parameters of and empirical geometric relations in organic disulfides see: Higashi, L., Lundeen, M. and Seff, K., 1978, *J. Am. Chem. Soc.*, **100**, 8101–8106.

[74] For an expansive survey of Raman spectra and structural parameters of cystine-related disulfides see: Van Wart, H. E. and Scheraga, H. A., 1976, *J. Phys. Chem.*, **80**, 1812–1823.

[75] For a discussion of the chiroptical properties of disulfides see: Rauk, A., 1984, *J. Am. Chem. Soc.*, **106**, 6517–6524.

[76] Ranganathan, D., Haridas, V., Nagaraj, R. and Karle, I. L., 2000, *J. Org. Chem.*, **65**, 4415–4422.

[77] Extremely compressed disulfides with r(S-S) shorter than the shortest reported S-S bond (FSSF *vide infra*) should be regarded with great skepticism and may solely be the result of crystal packing forces.

[78] Van Wart, H. E., Shipman, L. L. and Scheraga, H. A., 1975, *J. Phys. Chem.*, **79**, 1428–1435.

[79] Snyder, J. P. and Jørgensen, F. S., 1979, *Tetrahedron*, **35**, 1399–1407.

[80] Karle, I. L., Estlin, J. A., Britts, K., 1967, *Acta Crystallogr. Sect. A*, **22**, 273–280.

[81] Harpp, D. N., Priefer, R., Lee, Y. J., Barrios, F., Wosnick, J. H., Lebuis, A.-M., Farrell, P. G., Sun, A., Wu, S. and Snyder, J. P., 2002, *J. Am. Chem. Soc.*, **124**, 5626–5627.

[82] Snyder, J. P., Jørgensen, F. S. and Rindorf, G., 1980, *J. Org. Chem.*, **45**, 5343–5347.

[83] Snyder, J. P. and Jørgensen, F. S., 1980, *J. Org. Chem.*, **45**, 1015–1020.

[84] Lee, J. D. and Bryant, M. W. R., 1969, *Acta Crystallogr. Sect. B*, **25**, 2497–2504.

[85] Bernal, I. and Ricci, J. S., 1966, *Acta Crystallogr. Sect. A*, **21**, S104.

[86] Ostrowski, M., Jeske, J., Jones, P. G. and du Mont, W.-W., 1993, *Chem. Ber.*, **126**, 1355–1369.

[87] Raghavan, N. V. and Seff, K., 1977, *Acta Crystallogr. Sect. B*, **33**, 386.

[88] Ricci, J. S. and Bernal, I., 1969, *Acta Crystallogr. Sect. A*, **25**, S149.

[89] Shefter, E. and Kalman, T. I., 1969, *J. Chem. Soc. Chem. Commun.*, 1027–1029.

[90] Ricci, J. S. and Bernal, I., 1969, *J. Am. Chem. Soc.*, **91**, 4078–4082.

[91] Woodard, C. M., Brown, D. S., Lee, J. D. and Massey, A. G., 1976, *J. Organomet. Chem.*, **121**, 333–344.

[92] Lee, J. D. and Bryant, M. W. R., 1970, *Acta Crystallogr. Sect. B*, **26**, 1729.

[93] Furberg, S. and Solbakk, J., 1973, *Acta Chem. Scand.*, **27**, 2536–2542.

[94] Higashi, L., Lundeen, M. and Seff, K., 1978, *J. Am. Chem. Soc.*, **100**, 8101–8106.

[95] Shefter, E., Kotick, M. P. and Bardos, T. J., 1967, *J. Pharm. Sci.*, **56**, 1293–1299.

[96] Shefter, E. and Kalman, T. I., 1968, *Biochem. Biophys. Res. Commun.*, **32**, 878–884.

[97] Shefter, E., 1970, *J. Chem. Soc. B*, **5**, 903–906.

[98] Rosenfield, Jr, R. E. and Parthasarathy, R., 1975, *Acta Crystallogr. Sect. B*, **31**, 462–468.

[99] Oughton, B. M. and Harrison, P. M., 1959, *Acta Crystallogr.*, **12**, 396–404.

[100] Foss, O., Hordvik, A. and Sletten, J., 1966, *Acta Chem. Scand.*, **20**, 1169–1171.

[101] Hordvik, A., 1966, *Acta Chem. Scand.*, **20**, 1885–1891.

[102] Snyder, J. P. and Carlsen, L., 1977, *J. Am. Chem. Soc.*, **99**, 2931–2942.

[103] Fraser, R. R., Boussard, G., Saunders, J. K. and Lambert, J. B., 1971, *J. Am. Chem. Soc.*, **93**, 3822–3823.

[104] Benassi, R., Fiandi, G. L. and Taddei, F., 1997, *J. Mol. Struct. (THEOCHEM)*, **418**, 127–138.

[105] Kessler, H. and Rundel, W., 1968, *Chem. Ber.*, **101**, 3350–3357.

[106] The trend for calculated torsional barriers especially shows an increase in the cis barrier height.

[107] Hirota, E., 1958, *Bull. Chem. Soc. Jpn.*, **31**, 130–138.

[108] Kniep, R., Korte, L. and Mootz, D., 1983, *Z. Naturforsch. B*, **38**, 1–6.

[109] Ackermann, P. G. and Mayer, J. E., 1936, *J. Chem. Phys.*, **4**, 377–381.

[110] Palmer, K. J., 1938, *J. Am. Chem. Soc.*, **60**, 2360–2369.

[111] Beagley, B., Eckersley, G. H., Brown, D. P. and Tomlinson, D., 1969, *Trans. Faraday Soc.*, **165**, 2300–2307.

[112] Bock, H. and Solouki, B., 1977, *Inorg. Chem.*, **16**, 665–669.

[113] Brown, R. D., Marsden, C. J. and Godfrey P. D., 1979, *J. Chem. Soc. Chem. Commun.*, 399–401.

[114] Kuczkowski, R. L., 1964, *J. Am. Chem. Soc.*, **86**, 3617–3621.

[115] Marsden, C. J., Oberhammer, H., Losking, O. and Willner, H., 1989, *J. Mol. Struct.*, **193**, 233–245.

[116] Solà, M., Mestres, J., Carbó, R. and Duran, M., 1994, *J. Am. Chem. Soc.*, **116**, 5909–5915.

[117] Torrent, M., Duran, M. and Sola, M., 1996, *J. Mol. Struct. (THEOCHEM)*, **362**, 163–173.

[118] Bowen, H. J. M., 1954, *Trans. Faraday Soc.*, **50**, 452–463.

[119] Steudel, R., 1971, *Z. Naturforsch. B*, **26**, 750–756.

[120] Blaschette, A., Näveke, M. and Jones, P. G., 1991, *Z. Naturforsch. B*, **46**, 5–14.

[121] Das, D. and Whittenburg, S. L., 1999, *J. Phys. Chem. A*, **103**, 2134–2140.

[122] Jursic, B. S., 1996, *J. Comput. Chem.*, **17**, 835–840.

[123] Alleres, D. R., Cooper, D. L., Cunningham, T. P., Gerratt, J. and Karadakov P. B., 1995, *J. Chem. Soc. Faraday Trans.*, **91**, 3357–3362.

[124] Jursic, B. S., 1996, *J. Mol. Struct. (THEOCHEM)*, **366**, 97–103.

[125] Steudel, R. and Miaskiewicz, K., 1991, *J. Chem. Soc. Dalton Trans.*, 2395–2399.

[126] Koritsanszky, T., Buschmann, J., Schmidt, H. and Steudel, R., 1994, *J. Phys. Chem.*, **98**, 5416–5421.

[127] Steudel, R., Schmidt, H., Baumeister, E., Oberhammer, H. and Koritsanszky, T., 1995, *J. Phys. Chem.*, **99**, 8987–8993.

[128] Borghi, R., Lunazzi, L., Placucci, G., Cerioni, G., Foresti, E. and Plumitallo, A., 1997, *J. Org. Chem.*, **62**, 4924–4937.

[129] Tardif, S., 1997, The chemistry of dialkoxy disulfides and related compounds. PhD thesis, Montreal: McGill University.

[130] Harpp, D. N., Priefer, R. and Farrell, P. G., 2002, *Tetrahedron Lett.*, **43**, 8781–8784.

[131] Harpp, D. N., Zysman-Colman, E., Nevins, N. and Snyder, J. P., 2004, manuscript in preparation.

[132] Harpp, D. N. and Zysman-Colman, E., 2003, *J. Org. Chem.*, submitted.

[133] Snyder, J. P., Nevins, N., Tardif, S. L. and Harpp, D. N., 1997, *J. Am. Chem. Soc.*, **119**, 12685–12686.

[134] Turnbull, K. and Kutney, G. W., 1982, *Chem. Rev.*, **82**, 333–357.

[135] Kutzelnigg, W., 1984, *Angew. Chem. Int. Ed. Engl.*, **23**, 272–295.

[136] Foss, O., 1961, in: Organic sulfur compounds, Kharasch, N., (Ed.) (New York: Pergamon Press), pp. 75–96.

[137] Foss, O., 1950, *Acta Chem. Scand.*, **4**, 404–415.

[138] For a review on compounds containing the S=S bond see: Turnbull, K. and Kutney, G. W., 1982, *Chem. Rev.*, **82**, 333–357.

[139] Green, A. C., 1919, *J. Soc. Chem. Ind. London*, **38**, 459R.

[140] Gerbaux, P., Salpin, J.-Y., Bouchouxb, G. and Flammang, R., 2000, *Int. J. Mass Spectrom*, **195/196**, 239–249.

[141] Steudel, R., 1968, *Z. Anorg. Allg. Chem.*, **361**, 180–194.

[142] Steudel, R., 1972, *Z. Naturforsch. B*, **27**, 469–470.

[143] Schleyer, P. v. R., Bickelhaupt, F. M. and Solà, M., 1995, *J. Comput. Chem.*, **16**, 465–477.

[144] Stevenson, D. P. and Beach, J. Y., 1938, *J. Am. Chem. Soc.*, **60**, 2872–2876.

[145] Van Wart, H. E., Cardinaux, F. and Scheraga, H. A., 1976, *J. Phys. Chem.*, **80**, 625–630.

[146] Kushner, L. M., Gorin, G. and Smyth, C. P., 1950, *J. Am. Chem. Soc.*, **72**, 477–479.

[147] Steudel, R., Steudel, Y. and Miaskiewicz, K., 2001, *Chem. Eur. J.*, **7**, 3281–3290.

[148] Still, I. W. J., Reed, J. N. and Turnbull, K., 1979, *Tetrahedron Lett.*, **20**, 1481–1484.

[149] Baechler, R. D. and Daley, S. K., 1978, *Tetrahedron Lett.*, **19**, 101–104.

[150] Still, I. W. J., Hasan, S. K. and Turnbull, K., 1977, *Synthesis*, 468–469.

[151] Still, I. W. J., Hasan, S. K. and Turnbull, K., 1978, *Can. J. Chem.*, **56**, 1423–1428.

[152] Baechler, R. D., Daley, S. K., Daly, B. and McGlynn, K., 1978, *Tetrahedron Lett.*, **19**, 105–108.

[153] Bálint, J., Rákosi, M. and Bognár, R., 1979, *Phosphorus Sulfur*, **6**, 23.
[154] Baechler, R. D., San Filippo, L. J. and Schroll, A., 1981, *Tetrahedron Lett.*, **22**, 5247–5250.
[155] Oae, S., Yagihara, T. and Okabe, T., 1972, *Tetrahedron*, **28**, 3203–3216.
[156] Oae, S., Nakanishi, A. and Tsujimoto, N., 1972, *Tetrahedron*, **28**, 2981–2990.
[157] Still, I. W. J. and Turnbull, K., 1978, *Synthesis*, 540–541.
[158] Micetich, R. G., 1976, *Tetrahedron Lett.*, **17**, 971–974.
[159] Cookson, R. C. and Parsons, P. J., 1978, *J. Chem. Soc. Chem. Commun.*, 822–824.
[160] Baechler, R. D., Hummel, J. P. and Mislow, K., 1973, *J. Am. Chem. Soc.*, **95**, 4442–4444.
[161] Höfle, G. and Baldwin, J. E., 1971, *J. Am. Chem. Soc.*, **93**, 6307–6308.
[162] Exclusion of other mechanistic possibilities in the thermal isomerization of allyl-S_n-allyl and derivatives thereof, wherein $n = 2, 3$, is covered in detail in: Tidd, B. K., 1971, *Int. J. Sulfur Chem. C*, **6**, 101–107. Here it has been demonstrated that allylically unsaturated di- and trisulfides readily undergo a thermal [1,5]-sigmatropic rearrangement that results in cis,trans-isomerization of substituted compounds.
[163] Challenger, F. and Greenwood, D., 1950, *J. Chem. Soc.*, 26–30.
[164] Green, M., Lown, E. M. and Strausz, O. P., 1984, *J. Am. Chem. Soc.*, **106**, 6938–6946.
[165] Brandt, G. A. R., Emeleus, H. J. and Haszeldine, R. N., 1952, *J. Chem. Soc.*, 2198–2205.
[166] Stepanov, B. I., Rodionov, V. Y. and Chibisova, T. A., 1974, *J. Org. Chem. USSR (Engl. Transl.)*, **10**, 78–82.
[167] Drabowicz, J. and Oae, S., 1977, *Chem. Lett.*, 767–768.
[168] Soysa, H. S. D. and Weber, W. P., 1978, *Tetrahedron Lett.*, **19**, 235–238.
[169] Tebbe, F. N., Wasserman, E., Peet, W. G., Vatvars, A. and Hayman, A. C., 1982, *J. Am. Chem. Soc.*, **104**, 4971–4972.
[170] Benson, S. W., 1978, *Chem. Rev.*, **78**, 23–43.
[171] Barnard, D., Houseman, T. H., Porter, M. and Tidd, B. K., 1969, *J. Chem. Soc. Chem. Commun.*, 371–372.
[172] Safe, S. and Taylor, A., 1970, *J. Chem. Soc. C*, 432–435.
[173] Wong, M. W., Steudel, Y. and Steudel, R., 2002, *Chem. Phys. Lett.*, **364**, 387–392.
[174] Kuczkowski, R. L. and Wilson, Jr., E. B., 1963, *J. Am. Chem. Soc.*, **85**, 2028–2029.
[175] Kuczkowski, R. L., 1963, *J. Am. Chem. Soc.*, **85**, 3047–3048.
[176] Seel, F. and Budenz, R., 1965, *Chem. Ber.*, **98**, 251–258.
[177] Seel, F., Gombler, W. and Budenz, R., 1970, *Liebigs Ann. Chem.*, **735**, 1–5.
[178] Pez, G. P. and Brown, R. D., 1967, *Aust. J. Chem.*, **20**, 2305–2313.
[179] Brown, R. D., Burden, F. R. and Pez, G. P., 1965, *J. Chem. Soc. Chem. Commun.*, 277–278.
[180] Gombler, W., Schaebs, J. and Willner, H., 1990, *Inorg. Chem.*, **29**, 2697–2698.
[181] Davis, R. W. and Firth, S., 1991, *J. Mol. Spectrosc.*, **145**, 225–235.
[182] Seel, F. and Budenz, R., 1963, *Chimia*, **17**, 355–356.
[183] Seel, F. and Gölitz, D., 1964, *Z. Anorg. Allgm. Chem.*, **327**, 32–50.
[184] Cao, X., Qiao, C. and Wang, D., 1998, *Chem. Phys. Lett.*, **290**, 405–408.
[185] Lösking, O., Willner, H., Baumgärtel, H., Jochims, H. W. and Rühl, E., 1985, *Z. Anorg. Allgm. Chem.*, **530**, 169–177.
[186] Cao, X., Qian, X., Qiao, C. and Wang, D., 1999, *Chem. Phys. Lett.*, **299**, 322–326.
[187] A barrier of 36.7 kcal mol^{-1} for this same isomerization mechanism has been calculated at the MP2/6-31+G* level: Snyder, J. P. and Harpp, D. N. unpublished results.
[188] Allred, A. L. and Rochow, E., 1958, *J. Inorg. Nucl. Chem.*, **5**, 264–268.
[189] Reid, E. E., Macy, R., Jarman, G. N. and Morrison, A., 1947, *Science*, 355–359.
[190] Spong, A. H., 1934, *J. Chem. Soc.*, 485–492, and references cited therein.
[191] Amaresh, R. R., Lakshmikantham, M. V., Baldwin, J. W., Cava, M. P., Metzger, R. M. and Rogers, R. D., 2002, *J. Org. Chem.*, **67**, 2453–2458.
[192] Gerding, H., 1948, *J. Chim. Phys.*, **46**, 118–119.
[193] Bradley, E. B., Mathur, M. S. and Frenzel, C. A., 1967, *J. Chem. Phys.*, **47**, 4325–4329.
[194] Frankiss, S. G., 1968, *J. Mol. Struct.*, **2**, 271–279.
[195] Steudel, R., Jensen, D. and Plinke, B., 1987, *Z. Naturforsch. B*, **42**, 163–168.
[196] Frenzel, C. A. and Blick, K. E., 1971, *J. Chem. Phys.*, **55**, 2715–2719.
[197] Colton, R. J. and Rabalais, J. W., 1974, *J. Electron. Spectrosc. Relat. Phenom.*, **3**, 345–357.
[198] Stoll, O. and Scheibe, G., 1938, *Ber.*, **71**, 1571–1575.
[199] Yao, M., Kawakita, Y., Takahiro, S., Yamamoto, I. and Endo, H., 1997, *J. Phys. Soc. Jpn.*, **66**, 3115–3119.
[200] Chadwick, B. M., Grzybowski, J. M. and Long, D. A., 1978, *J. Mol. Struct.*, **48**, 139–142.
[201] Feuerhahn, M. and Vahl, G., 1979, *Chem. Phys. Lett.*, **65**, 322–323.
[202] Das, D. and Whittenburg, S. L., 1993, *J. Phys. Chem. A*, **103**, 2134–2140.
[203] Steudel, R., Schmidt, H., Sülzle, D. and Schwarz, H., 1992, *Inorg. Chem.*, **31**, 941–944.

[204] Using NRMS, HOSSOH is stable for only 10^{-5} s under highly dilute conditions in the gas phase.
[205] Thompson, Q. E., Crutchfield, M. M., Dietrich, M. W. and Pierron, E., 1965, *J. Org. Chem.*, **30**, 2692–2696.
[206] Steudel, R. and Schmidt, H., 1990, *Z. Naturforsch. B*, **45**, 557–558.
[207] Harpp, D. N., Tardif, S. L. and Williams, C. R., 1995, *J. Am. Chem. Soc.*, **117**, 9067–9068.
[208] Harpp, D. N., Nevins, N., Snyder, J. P. and Zysman-Colman E., manuscript in preparation.
[209] Steudel, R., Gleiter, R., Hyla-Kryspin, I. and Schmidt, H., 1993, *Chem. Ber.*, **126**, 2363–2365.
[210] HSOH is significantly more stable than $H_2S{=}O$. See: Wallmeier, H. and Kutzelnigg, W., 1979, *J. Am. Chem. Soc.*, **101**, 2804–2814.
[211] Harpp, D. N., Zysman-Colman, E. and Abrams, C. B., 2003, *J. Org. Chem.*, **68**, 7059–7062.
[212] Harpp, D. N., Steliou, K. and Cheer, C. J., 1980, *J. Chem. Soc. Chem. Commun.*, 825–826.
[213] Tanaka, S., Sugihara, Y., Sakamoto, A., Ishii, A. and Nakayama, J., 2003, *J. Am. Chem. Soc.*, **125**, 9024–9025.